A point mutation in the AF-2 domain of thyroid hormone receptor alpha1 expressed after CRE mediated recombination partially recapitulates hypothyroidism.

Laure Quignodon, Séverine Vincent, Harald Winter, Jacques Samarut, Frédéric Flamant

A point mutation in the AF-2 domain of thyroid hormone receptor alpha1 expressed after CRE mediated recombination partially recapitulates hypothyroidism.

Short title: TRα1 dominant negative mutation in mice.

Laure Quignodon, Séverine Vincent, Harald Winter*, Jacques Samarut, Frédéric Flamant** Institut de Génomique Fonctionnelle de Lyon ; Université de Lyon; Institut Fédératif Biosciences Gerland Lyon Sud; Université Lyon 1, CNRS, INRA, Ecole Normale Supérieure de Lyon, France. * University of Tübingen, Tübingen Hearing Research Centre, Laboratory of Molecular Neurobiology

**Corresponding Author: To whom correspondence and proof should be sent
Institut de Génomique Fonctionnelle
Ecole Normale Supérieure de Lyon
46 allée d'Italie 69364 Lyon CEDEX 07
Tel: 00 (33) 4 72 72 86 21 FAX: 00 (33) 4 72 72 80 80
Frederic.Flamant@ens-lyon.fr

Keywords: Thyroid hormone receptor/ transgenic mice/development

Disclosure of Potential Conflict of Interest Form : Authors have nothing to declare.

Abbreviations footnote: Q-RT-PCR: quantitative-reverse transcription-polymerase chain reaction.

ABSTRACT

Thyroid hormones act directly on transcription by binding to TRα1, TRβ1, TRβ2 nuclear receptors, regulating many aspects of post-natal development and homeostasis. To precisely analyze the implication of the widely expressed TRα1 isoform in this pleiotropic action, we have generated transgenic mice with a point mutation in the TRα1 coding sequence, which is expressed only after CRE/loxP mediated DNA recombination. The amino-acid change prevents interaction between TRα1 and histone acetyltransferase coactivators and the release of corepressors. Early expression of this dominant-negative receptor deeply affects post-natal development and adult homeostasis, recapitulating many aspects of congenital and adult hypothyroidism, except in tissues and cells where TRβ1 and TRβ2 are predominantly expressed. Both respective abundance and intrinsic properties of TRα1 and TRβ1/2 seems to govern specificity of action.

INTRODUCTION

Thyroid hormones (TH) consist in 3,5,3'-tri-iodothyroinine (T3) and its precursor thyroxine (T4) which displays a weaker biological activity. Both molecules are secreted by thyroid gland follicles, but most of T3 synthesis results from T4 deiodination in other organs. T3 binds to nuclear receptor (TRs) present as three different isoforms, TRα1, TRβ1, TRβ2 encoded by the two *THRA* and *THRB* genes. TRs bind in a ligand-independent manner to specific response elements, mainly as RXR heterodimers, which are widespread in the genome. Unliganded TRs recruit transcription corepressors. Among these NcoR and SMRT function as platforms for the recruitment of histone deacetylases. T3 binding results in a displacement of the C-terminal helix of TR, which contains activation function 2 (AF-2). This permits the recruitment of several coactivators complexes, some of them, like SRC1 and SRC2, having a histone acetyl-transferase activity (1, 2) and destabilizes interactions with histone deacetylase corepressors.

TH signaling exerts multiple effects on post-natal development and the maintenance of homeostasis in adults by directly regulating target gene transcription (3). Previous investigations used various strategies to decrease TH levels. Among several animal models, transgenic mice recently gained popularity, at the expense of thyroidectomized or pharmacologically manipulated rats. In *Pax8*$^{-/-}$ knockout mice, the only reported primary defect is the absence of thyroid follicular cells (4). Although these animals can receive maternal TH through placenta during fetal development, they usually die within three weeks after birth, unless they are rescued by TH treatment. The direct and indirect effects of congenital hypothyroidism are difficult to unravel. TR knockouts mice offered new possibilities to solve this problem and allowed attributing specific function to each receptor isoform

(5). The broadly expressed TRα1 appears to be the main regulator of development during the first three weeks of post-natal, pre-weaning development. This period, somewhat reminiscent of amphibian metamorphosis (6), is marked by a transient increase in TH circulating level. At this time, liganded TRα1 regulates intestinal remodeling (7), cerebellum development (8), spleen erythropoiesis (9) and bone growth (10). TRα1 has a later role in setting cardiac function (11) and thermogenesis. TRβ1 and TRβ2 expression pattern is more restricted. These isoforms are the main regulators of liver function, inner ear development, retinal cones differentiation, and feedback regulation of the hypothalamic-pituitary-thyroid axis.

Surprisingly the deletion of all TR isoforms, obtained by the combination of *THRA* and *THRB* knockouts, is not lethal and only partially recapitulates the post-natal consequences of congenital hypothyroidism observed in *Pax8*$^{-/-}$ mice (12, 13). Several studies support the hypothesis that this discrepancy is due to the negative effect exerted by the unliganded TRα1 present in hypothyroid *Pax8*$^{-/-}$ mice, but not in *THRA/THRB* knockout mice. In line with this, the consequences of TH depletion are attenuated when *THRA* is deleted (8, 14). Furthermore the consequences of *THRA* knockout are limited compared to those of *THRA* knock-in mutations. Three germline knock-in mutations have been introduced in the ligand binding domain of TRα1. The reading frame mutations have different consequences on ligand binding and cofactor interactions, but all preserve DNA binding and reduce the transcriptional activation ability of TRα1. Mice heterozygous for these mutations display many features of congenital hypothyroidism, suggesting a constitutive repression of TH target genes (15-18). The hypothesis that congenital hypothyroidism is mainly due to the negative action of unliganded TRα1 remains however controversial for several reasons. First, the rescue of *Pax8*$^{-/-}$ mice by *THRA* knockout is only partial, and not observed with all *THRA* alleles (19). Another difficulty is that the consequences of the three *THRA* knock-in mutations are not identical. For example, obesity has been reported in only one case. For these reasons, several additional hypothesis have been proposed, including the intervention in hypothyroid mice of unliganded TRβ (20), of TRα2, a *THRA* encoded isoform which is unable to bind T3 (19), or of TH non-genomic effects (21, 22).

We describe here the construction of a new mouse allele for the *THRA* gene, encoding a TRα1 receptor with an AF-2 mutation (L400R). According to structural data, the mutation fills a cavity at the surface of the ligand binding domain which is required for histone acetyl transferase coactivators interaction. The mutation prevents histone acetyl transferase recruitment and favours the permanent recruitment of corepressors. This is responsible for a dominant negative activity exerted on both TRα1 and TRβ receptors in transient expression assays. The genetic construct introduced by homologous recombination in the *THRA* locus possesses an upstream floxed cassette, allowing for a spatio-temporal expression control of TRα1^{L400R} expression, using the Cre/loxP recombination system. The

phenotypic consequences of an early embryonic recombination of this *THRA* allele on development and homeostasis closely resemble those of congenital and adult hypothyroidism, except in tissues where *THRB* function is predominant. We conclude that, although hypothyroidism manifestations mainly results from to the negative action of the ubiquitous unliganded TRα1, unliganded TRβ also contribute in several tissues.

RESULTS

Construction of the *TRa*^{AMI} allele

We introduced in the AF-2 domain of the mouse TRα1 receptor a point mutation converting a leucine into an arginine (L400R) equivalent to the L454R mutation previously created in the human TRβ1 (23, 24). It has been shown previously that this TRβ1 mutation fully prevents interaction with the histone acetyl transferase coactivators while preserving interaction with histone deacetylase corepressors (34), resulting in a very strong dominant-negative activity on TR mediated transactivation. Recently, this mutation has also been shown to prevent an interaction between AF-2 and the hinge region, but the functional significance of this interaction remains unclear (25). We verified, using a proteolysis sensitivity assay, that ligand binding was not abolished by the mutation (data not shown). We used yeast two-hybrid assays to confirm that, whether T3 is present or not, TRα1^{L400R} interacts with the NcoR histone deacetylase corepressor but not with the SRC1 or SRC2 histone acetyl transferase coactivators (Figure 1A). We then introduced the TRα1^{L400R} cDNA between two cassettes. The downstream *IRESTaulacZ* cassette encodes a β-galactosidase targeted to the cytoskeleton, translated from an ECMV internal ribosomal entry site. We placed the entire construct downstream to a CMV transcription promoter (figure 1B) to perform transient expression assays. The upstream *PGKNeoRpolyA* cassette confers G418 resistance to eukaryotic cells and contains a SV40 polyadenylation signal, which arrests most transcription and prevents any TRα1^{L400R} translation. As the upstream *PGKNeoRpolyA* cassette is flanked by two tandem *loxP* sequences, CRE mediated recombination is required to produce a bicistronic mRNA encoding both TRα1^{L400R} and β-galactosidase. This design was expected to favor the detection of recombination events in mouse tissues by Xgal staining. Transient expression results confirm that synthesis of both TRα1^{L400R} protein (Figure 1C) and β-galactosidase (data not shown) requires previous excision of the *PGKNeoRpolyA* cassette. TRα1^{L400R} was not able to activate transcription via a T3 response elements (2xDR4), and exerted a strong dominant negative effect on transcriptional activation mediated by the wild-type liganded TRα1 receptor (Figure 1D). A similar dominant-negative action was observed when TRβ1 or TRβ2 was used for transactivation (data not shown). All these observations lead to the conclusion that the L400R mutation places the TRα1 receptor in a conformation, equivalent to the unliganded state, that exert a constitutive dominant-negative effect on TR target genes expression.

The TRα1^{L400R} reading frame flanked by the upstream *PGKNeoRpolyA* and the downstream *IRESTaulacZ* cassettes, was introduced in the mouse *THRA* locus by homologous recombination (Figure 2A,B). In the resulting *TRa^{AMI}* allele (AF-2 Mutation, Inducible), the mutation is silent. CRE recombination is required to express TRα1^{L400R} from its natural promoter, at a level similar to the endogenous TRα1 receptor. To address the ability of ES cells to express *TRα1^{L400R}* after CRE recombination, CRE was transiently expressed in *TRa^{AMI}*/+ ES cells and RT-PCR was performed to amplify the 3' part of the TRα1 cDNA. As *TRα1^{L400R}* cDNA differs from its wild-type counterpart by the presence of a SacII restriction site we digested the PCR product with SacII and confirmed by gel electrophoresis the presence of both type of mRNA in *TRa^{AMI}*/+ ES cells after CRE recombination (Figure 2C). ES cells carrying an intact *TRa^{AMI}* allele were injected into blastocytes to produce mouse chimeras. After germline transmission, *TRa^{AMI}*/+ mice, which express only one intact THRA allele, were obtained. They displayed, as expected, a normal growth and fertility and an apparently normal phenotype. *TRa^{AMI}/TRa^{AMI}* animals, which do not express any *THRA* isoforms, were obtained at the next generation. These homozygous animals, whose phenotype was not investigated, were able to develop and breed normally, like other *THRA* knockout mice.

Early and ubiquitous expression of TRα1^{L400R} leads to a hypothyroid-like phenotype

To trigger a broad expression of TRα1^{L400R} we crossed *TRa^{AMI}*/+ mice with *SYCP1CRE* transgenic mice. These mice have been reported to express the CRE recombinase only during male spermatogenesis (26). We thus expected *TRa^{AMI}*/+*xSYCP1CRE* males to give rise to progenies where a deleted *TRa^{AMI}* allele would be in all cells from the beginning of development, and TRα1^{L400R} expressed ubiquitously. Unlike previous reports, we found that complete excision did not occur in all cases, some *TRa^{AMI}*/+*xSYCP1CRE* males giving rise to offspring with no or partial excision. To circumvent this problem, probably due to variegation in CRE expression, we selected favorable *TRa^{AMI}*/+*xSYCP1CRE* males for further experiments and only considered pups with excision efficiency, as evaluated by PCR, superior to 90% (Figure 3A). We will call these heterozygous mice, which express *TRα1^{L400R}* in most tissues, *TRa^{AMI}xS*. We performed RT-PCR to demonstrate the presence of a SacII containing *TRα1^{L400R}* cDNA in several tissues (data not shown). Q-RT-PCR was also used to evaluate the total expression level of *TRα1* (*TRα1^{L400R}*+wild-type) in *TRa^{AMI}xS* mice. The expression level at P15 was similar to the one observed in wild type animal in liver with a 3-fold increase in the cerebellum (Table I) and brain (data not shown). This slight augmentation could result from the absence of alternate splicing in the *TRa^{AMI}* locus, a phenomenon that normally diverts part of the *THRA* transcription to produce TRα2, an isoform which does not bind T3. β-galactosidase activity was very weak or undetectable, probably due to low expression level of the *THRA* locus, and perhaps to limited efficiency of translation initiation at the IRES element.

At P15 the fraction of *TRa*^{AMI}*xS* in litters was close to the expected 50% ratio. It seems therefore that expression of the *TRα1*^{L400R} expression is compatible with pre-natal and early post-natal development of heterozygous mice. By contrast later development was deeply affected, and 48% of the *TRa*^{AMI}*xS* pups did not reach the adult age (N=61). The development of surviving mice was strongly delayed. Eye opening did not occur before P25, compared to an average of P15 for wild-type littermates. Body growth was greatly reduced (Figure 3B). This correlated with delayed ossification of long bones (Figure 3C), and reduced growth hormone gene expression level in pituitary gland (Table I). After weaning, the body weight of the surviving mutant mice increased, but the adults suffered from permanent and disproportioned dwarfism. Measurement of body fat content by nuclear magnetic resonance did not reveal any increase in adiposity (Table I) also intraperitonal content in white adipose tissues was found to be strongly reduced, when 4 weeks-old and 3 months-old animals where dissected. *TRa*^{AMI}*xS* females were sterile, without obvious histological defects in ovaries (data not shown).

Beside dwarfism, *TRa*^{AMI}*xS* animals displayed several other features of congenital hypothyroidism. This was the case in the spleen (Table I), whose weight was highly reduced at P15. In the cerebellum, the external granular layer, a transient structure which normally disappears at earlier stage, persisted at P21 (Figure 3D). The expression level of genes sensitive to hypothyroidism, *Hairless* in granular neurons and *Pcp2* in Purkinje cells was significantly reduced (Table I). Signs of cerebellar defect were also observed in adult *TRa*^{AMI}*xS* mice, which displayed a characteristic ataxia bearing, spreading their hindlimbs to maintain their posture. Adult *TRa*^{AMI}*xS* mice had reduced heart rate (Table I) and sometimes displayed cardiac arythmia. This cardiac phenotype correlated with a decreased expression at P15 for two T3 target genes, the potassium channel encoding genes *HCN2* and *KCNB1* (Table I). The body temperature was usually close to normal in *TR*^{AMI}*xS* mice (Table I). However, a cold tolerance test revealed, like in mice lacking all TR isoforms (27) a defect in thermogenesis ability, the body temperature of *TRa*^{AMI}*xS* mice dropping within few hours after cold exposure for a fraction of animals (Figure 3E). T3 and T4 levels were not changed in *TRa*^{AMI}*xS* mice (Table I). The previously observed phenotypic alterations, which are all reminiscent of hypothyroidism, are thus not indirect consequences of a central deregulation of TH secretion but consequences of peripheral *TRα1*^{L400R} expression.

TRβ expressing cells are less sensitive to *TRα1*^{L400R} expression

Previous genetic analysis underlined a predominant function of TRβ1 and TRβ2 receptors in several TH functions, including feedback-regulation of TSH secretion from pituitary thyrotropes and metabolic control in hepatocytes. TRβ1 is also involved in inner ear hair cells, retina cones and cerebellum Purkinje cells differentiation. Whether this results from predominant expression of *THRB*

over *THRA* in these cell types or from intrinsic properties of TRβ receptors is unclear. Circulating level of TSH (data non shown) and *TSHβ* expression in pituitary (Table I) were not significantly affected at P15 in *TRa^{AMI}xS* mice. In liver, Q-RT-PCR failed to demonstrate a significant change in expression level for two TH target genes at P15: *Dio1,* encoding type 1 deiodinase and *Me3*, encoding the NADP dependent malic enzyme (Table I). Similarly, Q-RT-PCR measurement of opsin gene expression failed to reveal a loss of M-Opsin cones in retina (data not shown), suggesting that, unlike *TRβ* knockout mice, *TRa^{AMI}xS* are not colour blind. Purkinje cells differentiation was addressed by observing dendritic arborization after calbindin-D28k immunostaining and by measuring *Pcp2* mRNA level in cerebellum. These two parameters revealed a defect in differentiation at P15 (Figure 3F, table I). However, unlike what is reported for hypothyroid animals, this was followed by an apparent recovery at P21 (data not shown). TRβ1 function was also analyzed in the inner ear. Interestingly, it has been shown previously that, in outer hair cells, TRα1 and TRβ1 can fulfill distinct functions. TRα1 regulates *Kcnq4* a potassium channel, while TRβ1 activates *Slc26a5* expression, a gene encoding a motor protein called prestin (28). In line with this, immunocytochemistry revealed that the level of KCNQ4, but not of prestin, was highly reduced in *TRa^{AMI}xS* mice (figure 4). All these observations reveal that *TRa^{AMI}xS* mice do not display all the features of acute congenital hypothyroidism and that some TRβ prevalent functions are preserved.

Tamoxifen induction of *TRα1^{L400R}* expression.

In order to evaluate the possibility to perform a kinetic study of TRα1^{L400R} effect on development, we crossed *TRa^{AMI}*/+ mice with *CagCreER^{TM}* mice, that broadly express a modified CRE recombinase, which enzymatic activity is inducible by tamoxifen (29). The resulting heterozygous conditional mutants (*TRa^{AMI}xC*) were treated at E17.5 with tamoxifen. This resulted in the excision of the *PGKNeoRpolyA* cassette in most tissues. The excision efficiency varied from one tissue to the other (Figure 5A). In general the phenotype of tamoxifen treated *TRa^{AMI}xC* animals was similar to the one of *TR^{AMI}xS*, but less severe. This conclusion was based on observations of growth curves (Figure 5B), ossification at P15 (Figure 5C), cerebellum histology (Figure 5D), adult heart rate, expression level at P15 of *KCNB1* and *HCN2* in heart, and *Hairless* and *Pcp2* in cerebellum (Table I). This demonstrates that expression of TRα1^{L400R}, even when started at a late fetal stage, is sufficient to affect post-natal development. The relatively mild phenotype of tamoxifen treated *TRa^{AMI}xC* pups, compared to *TR^{AMI}xS,* might only reflect the incomplete excision of the floxed cassette. We also performed tamoxifen treatment in adult *TRa^{AMI}xC* mice, to overcome detrimental effect of early TRα1^{L400R} expression. This treatment did not have any visible effect in the short term cold tolerance assay, either because recombination efficiency was not sufficient in brown adipose tissue, or because the thermosensitive phenotype observed in *TRa^{AMI}xS* might result from a developmental alteration. Nevertheless, tamoxifen treatment of adult *TRa^{AMI}xC* males induced a significant reduction in heart

rate (Figure 3E) indicating that at least this last alteration is not a long term consequence of some developmental defect. *TRα^{AMI}xC* mice therefore appear as a suitable model to separate between the developmental and adult homeostatic function of TRα.

DISCUSSION

In this report we describe for the first time a CRE inducible system able to express a dominant negative mutation of TRα1^{L400R}. TRα1^{L400R} is equivalent to an unliganded TRα1 receptor, as it prevents interactions with histone acetyl transferase transcription coactivators in a highly specific manner, without compromising interaction with corepressors. The first practical advantage of CRE dependent expression is to permit an easy production of mutant offspring, as the mutated receptor is not expressed in breeding animals. This also rules out that the maternal expression of the mutation indirectly influences the development of pups. This is expected for example for neuronal migration in the cortex (30). This experimental design also opens a broad field for new investigations of TH signaling in mice, as the use of tissue specific promoter and of an inducible version of the CRE will permit to control the expression of TRα1^{L400R} during development and in adults. This will permit to separate between the direct and indirect effects of TH signaling, as illustrated here for the cardiac function. As a large number of mice expressing CRE or an inducible version of CRE, have been already generated worldwide (31), this appears as a highly flexible method to create new animals models. These animals will be specifically affected in one or several of the functions sensitive to TRα1^{L400R} expression, within only one generation time. These functions include, in addition to those studied above, lipid storage in white adipose tissue (32), intestinal maturation (33), early post-natal erythropoiesis (9), lymphopoiesis (34) muscle function (35), myelin formation (36) and regeneration (37), hearing onset (38) , adult brain stem cells proliferation (39, 40), anxiety control and memory (41).

Three other *THRA* knock-in mutations have been reported before, which affect the TRα1 ligand-binding domain in different manner. Unlike the TRα1^{L400R} mutation, whose design was based on structural considerations, the changes in the TRα1 reading frame were copied from *THRB* germline mutations found in patients with resistance to thyroid hormone. Comparisons between *TRα^{AMI}xS* and the previously reported *THRA* knock-in mouse strains enable to define constant features among the multiple consequences of expressing a dominant negative TRα1. As far as we can tell, the *TRα^{AMI}xS* mice phenotype appears to be very similar to those reported for mice carrying the *TRα1^{R384C}*, which reduces the affinity of the ligand binding domain for T3 (15) and the *TRα1^{PV}* mutation, a frameshift mutation resulting in the loss of the N-terminal AF-2 domain (16, 42, 43). The fourth reported knock-in mutation, *TRα1^{P398H}*, is the only one that induces obesity and not dwarfism. From our data, we can rule out that this peculiar phenotype results from the inability of TRα1^{P398H} to recruit histone acetyl

transferase coactivators or release corepressors. It has been suggested that *TRα1*^{P398H}/+ obesity rather results from a cross-talk between TRα1^{P398H} and PPARα in liver (44) (45). However a similar cross-talk with PPARγ in white adipocytes has been proposed to explain the opposite phenotype in *TRα1*^{PV}/+ mice (42). Many human germline point mutations that prevent histone acetyl transferase recruitment have been reported for *THRB,* but not for *THRA*. From these studies we can predict that an AF-2 mutation in the human TRα1 receptor would have dramatic consequences on development even at the heterozygous state.

The phenotypic similarities between *TRα*^{AMI}*xS* and *Pax8*$^{-/-}$ hypothyroid mice demonstrate that the ligand-mediated recruitment of histone acetylase coactivators and/or release of corepressors by TRα1 is crucial for post-natal development. This strengthens the previous conclusion that congenital hypothyroidism is mainly a manifestation of the negative action of unliganded TRα1 (14). However differences are found between *TRα*^{AMI}*xS* and *Pax8*$^{-/-}$ animals, suggesting a more complex situation. For example, the majority of *TRα*^{AMI}*xS* survive beyond weaning, while *Pax8*$^{-/-}$ mice usually die within three weeks after birth. Our data suggest that in cells where *THRB* is highly expressed, like thyrotropes, hepatocytes, and retina cones, liganded TRβ can balance the down-regulation exerted by TRα1^{L400R}. Such a compensation cannot take place in hypothyroid mice, where unliganded TRβ receptors might instead participate to negative gene regulation and further compromise post-natal development. The presence of liganded TRβ in *TRα*^{AMI}*xS* can explain all the differences observed with *Pax8*$^{-/-}$ hypothyroid mice, leaving little place for the proposed intervention of the antagonist TRα2 isoform (19) or of an hypothetical TR independent TH signaling pathway (21, 46). It seems therefore that unliganded TRα1, and to a lesser extent unliganded TRβ, can account for all the detrimental effects of hypothyroidism in juveniles and in adults.

One important question that our data can help to clarify is whether the individual functions of TRα1 and TRβ1/2 isoforms in a given cell type are dictated by their respective abundance or by differences in their intrinsic properties. A vast amount of *in vitro* data suggests that TRα1 and TRβ1/2 are, at least at first sight, functionally equivalent. Knockout observations strengthen this hypothesis, as the phenotypic differences observed between *THRA* and *THRB* individual knockouts mainly reflect their contrasting expression patterns. Combinations of *THRA* and *THRB* knockout mutations also suggest functional redundancy, as several phenotypic alterations augmented (3, 47). As expected TRα1^{L400R} exerts in transient expression assays a dominant-negative action both on TRα1 and TRβ1. Accordingly, most features of the *TRα*^{AMI}*xS* phenotype can be predicted from the respective abundance of *THRA* and *THRB* encoded receptors in a given cell type. First, we failed to detect any phenotypic alteration in cell types known to express *THRB* at much higher level than *THRA*. This includes retina cones, hepatocytes and thyrotrope cells. Second, TRβ receptors appear sensitive to the TRα1^{L400R}

dominant-negative effect in tissues where the stochiometry is less favorable to *THRB*. Previous genetic studies have shown that compound knockout mice devoid of all receptors have a reduced body temperature and are much more sensitive to cold exposure than *THRA* knockout mice (27, 48, 49). Thus, despite pharmacological evidences indicating only partial overlap (50), the functions of the two receptors seem to be redundant for cold resistance, correlating with the concomitant presence of TRα1 and TRβ1 in brown adipose tissue (51). The fact that *TRα^{AMI}xS* are highly sensitive to cold exposure therefore suggests that TRα1^{L400R} can interfere with both TRα1 and TRβ1 functions in brown adipocytes. A similar interpretation can be proposed for Purkinje cells. Hypothyroidism results in a permanent reduction in dendritic arborization and a disorganization of the cells alignment (52). *In situ* hybridization reveals a predominant *THRB* expression in these cells after birth (53), and their differentiation is deeply affected by a TRβ knock-in mutation (20). However, *in vitro* differentiation of purified Purkinje precursors rather suggests a predominant function for TRα1 over TRβ1 (54). We show here that *TRα1^{L400R}*, like *TRα1^{R384C}* (41) has only a transient effect on Purkinje dendrites arborization. A possible explanation would be that, as *THRB* expression increases over time in this cell type (55), TRβ1 progressively accumulates, overcomes the transcription repression exerted by *TRα1^{L400R}* and eventually unlocks differentiation. In conclusion, expression patterns clearly influence the respective *in vivo* function of TRα1 and TRβ1/2. TR stochiometry is however unlikely to be the only explanation for the maintenance of several TRβ1/2 dependent functions in *TRα^{AMI}xS* mice. Some our results also suggest that TRα1 and TRβ1/2 intrinsic properties, and the set of target genes that they control, are different. For example, the resting body temperature of most *TRα^{AMI}xS* animals is normal, unlike what is reported for compound *THRA/THRB* knockout mice, suggesting that part of the activation by TRβ1 is preserved in brown adipocytes. Most importantly, the inner ear phenotype provides compelling evidence that TRα1 and TRβ1 intrinsic properties are different. Within outer hair cells, *TRα1^{L400R}* appears to antagonize TRα1 driven transactivation of KCNQ4 without compromising TRβ1 mediated regulation of prestin. It seems therefore that in vertebrates, divergent evolution of the paralogous *THRA* and *THRB* genes increased the variety of cellular responses to TH.

MATERIAL AND METHODS

Plasmids and transient expression assays

The L400R mutation was introduced in the TRα1 reading frame present in the pBIRDTRα1 construct (56) using for PCR mutagenesis an oligonucleotide containing a SacII restriction site at the mutation site: 5' CC CCG C*GG* TTC CTG GAG GTC TTT GAG 3'. The entire cDNA structure was confirmed by DNA sequencing. The mutated cDNA was inserted between a floxed *PGKNeoRpolyA* (57) able to stop transcription, and an *IRESTaulacZ* sequence (58) to create a bicistronic mRNA encoding both the mutated receptor TRα1^{L400R} and the reporter Tau-β-galactosidase fusion protein targeted to the

cytoskeleton. The completed construct was transferred as a PacI restriction fragment into the pBK-CMV expression vector (Stratagene San Diego) (figure 1B) or between two large genomic fragments (Figure 2A) cloned into the Supercos1 cosmide vector (Stratagene) for homologous recombination. An identical pBK-CMV derivative was made for the intact TRα1 cDNA for control experiments. For transient expression, Cos-7 cells, maintained in TH depleted medium, were transfected with Exgen reagent (Fermentas). pTK-DR4(2x)-luc was used as a reporter construct (59) and pRL-CMV (Promega), encoding renilla luciferase, as an internal standard. T3 (10^{-7}M) was eventually added to the medium 24h before the quantification of luciferase activity (Promega, Dual Luciferase Assay). The full-length TRα1 and TRα1^{L400R} reading frames were transferred into pAS2.1 (Clontech) to perform two-hybrid assays in yeast cells. Two-hybrid interactions were tested by plating AH109 yeast cells on selective medium and quantified by measuring β-galactosidase activity in Y187 yeast cells, using orthonitrophényl-β-D-galactopyrannoside as a substrate.

Generation of mutant mice

The oligonucleotides used for vector construct, screening and *TRα* expression analysis are the following (positions on figure 2). a: 5'GCGATACCGTAAAGCACGAG ; b : 5'GCCTTCTATCGCCTTCTTGACG ; c : 5'CGTCTGGAGAAGAGTTGG d : 5' TCCACAGGTATCTCCAGACAGG e : 5' GATTCTTCTGGATTGTGCGGCG f : ACCGCAAACACAACATTCCGCACTTCTGGC g : 5' GAGGAAGGAGAGAAGAGATG GGGGTTC h : 5' CGGTCGCTACCATTACC AGTTG i : 5' TTATGGATGGACGGACGG j : 5' AGTCTACGGCAAGGCAACACCAAG. 5x10^6 129/Sv mouse embryonic stem cells (13) were electroporated with 40 μg of linear plasmid and selected with G418 (250 μg/ml; Gibco-BRL). Cell clones were picked 10 days later and screened by PCR amplification of junction fragment, using Long expand Taq polymerase (Roche) (a+c for the 5' side, h+j for the 3' side). 3 out of 310 clones carried the mutant allele called *TRα^{AMI}*(*AF-2 Mutation, Inducible*). After further PCR characterization of the recombinant allele, cells were injected into C57/Bl6 blastocysts to generate chimeras. After germline transmission, transgenic mice were routinely screened by PCR directed on the lacZ – exon 9 junction (h+i). *TRα^{AMI}*xS and *TRα^{AMI}*xC mice were produced by crossing *TRα^{AMI}*/+ mice with *SYCP1CRE* transgenic mice (26) and *CagCreER^{TM}* (29) respectively and identified by PCR (5'TTACCGGTCGATGCAACG3'+ 5'CCAGCCACCAGCTTGCAT3' for CRE). When indicated, *TRα^{AMI}*/C mice received 1 (pregnant E17 mothers) or 5 (adults) daily intra-peritoneal injection of tamoxifen (Sigma T-5648, 50 mg/kg) dissolved in corn oil. CRE mediated deletion was identified by PCR (b+d+e). All animals experimentations were performed under Animal care procedures and conducted in accordance with the guidelines set by the European Community Council Directives (86/609/EEC).

Phenotype analysis

RNA were extracted from tissues of 8-10 mice per group and purified using RNeasy (Qiagen) or RNA Nanoprep (Stratagene) extraction kits, including a DNaseI treatment. RNA quality controls were performed by gel electrophoresis (Agilent 2100 Bioanalyzer). cDNA were prepared from 1 µg RNA using M-MLV reverse transcriptase (Promega) and random 6-mers primers. After 1/40 dilution, 2 µl of cDNA were used for quantitative PCR (Stratagene Mx3000P® QPCR System), using either Platinum® Quantitative PCR SuperMix (Invitrogen) or Taqman Assay-on-Demand (Applied Biosystems). Quantitation was performed in duplicates using the *HPRT* and *TBP* housekeeping genes as internal standards (or *ARBP* for pituitary) and the $2^{-\Delta\Delta Ct}$ method for data analysis (60). Parrafin sections were prepared from tissues fixed with 4% paraformaldehyde. Purkinje cells were stained with a rabbit anti-calbindin-D-28k antibody (Swant CB38a, 1/5000 dilution). Serum T4, T3 and TSH levels were measured as described previously (61). Cold tolerance assays were performed with a telemetry system as previously described (48) in a 4°C room. Body temperature was measured every 15 or 30 minutes during 8 hours and mice were removed from the cold room when their body temperature dropped below 35°C. Inner ear immunocytochemistry was performed as described previously (28).

Acknowledgements:

We thank Peggy Del Carmine and Michel Beylot from the ANIPHY facility for performing electocardiograms, Nadine Aguilera and the PBES breeding facility group for mouse breeding. We also thank Marlies Knipper and Karine Gauthier for helpful discussion and critical reading of the manuscript, Roy Weiss for TSH measurement, Martin Privalsky, Richard Axel, Denis Duboule and Nathalie Billon for plasmid gifts. This work was supported by the CASCADE European network of excellence and the CRESCENDO European integrated project. LQ was supported by Fondation pour la Recherche Médicale.

FIGURES

Figure 1: Properties of the TRα1^{L400R} mutated receptor

A: Two-hybrid interactions in yeast show that TRα1^{L400R} can only interact with corepressors. Unlike liganded TRα1, TRα1^{L400R} does not interact with SRC1 and SRC2 histone acetyl transferase coactivators. The interaction with the NcoR corepressor is ligand sensitive for TRα1 but constitutive for TRα1^{L400R}. B: Cytomegalovirus (CMV) and phospho-glycerate-kinase (PGK) promoters generate transcripts terminated by the SV40 polyadenylation signal present in the *PGKNeoRpolyA* cassette. The bicistronic TRα1^{L400R} and TaulacZ cDNA, located downstream to the SV40 polyadenylation signal, cannot be expressed. As the *PGKNeoRpolyA* cassette is flanked by two loxP sequences, CRE mediated deletion enables TRα1^{L400R} and TaulacZ synthesis. C: TRα1^{L400R} expression requires CRE mediated deletion. Western blotting of mammalian COS7 cells transfected with the CMV construct encoding for TRα1^{L400R} (1, 2) or the empty CMV construct (3). When the floxed *PGKNeoRpolyA* cassette is present (1), only a non-specific band is detected, reflecting the absence of TRα1^{L400R} expression. The CRE deleted construct (2) encodes the expected 44 kDa TRα1^{L400R} protein. D: TRα1^{L400R} acts as a dominant negative receptor. Transient luciferase expression in transfected COS7 cells show that, unlike wild-type TRα1, TRα1^{L400R} can not transactivate a DR4-TK-luc construct in the presence of T3. TRα1 mediated transactivation is antagonized by increasing amount of TRα1^{L400R}. A 1/1 ratio leads to a complete inhibition of T3 response.

Figure 2: Generation of the *TRa^{AMI}* allele by homologous recombination in mouse embryonic stem cells. A: Structure of the *THRA* locus after homologous recombination. From 5' to 3': *THRA* sequences absent from the recombination vector (black line) 6,5kb of *THRA* genomic sequences extending to the non coding part of exon2 (nucleotide 279 on Genebank # NC_000077 dark grey box); the *PGKNeoRpolyA* cassette, providing G418 resistance to ES cells, flanked by two tandem *loxP* for CRE mediated deletion; TRα1^{L400R} encoding sequence; *ECMV*-IRES element for internal ribosomal entry; *TaulacZ* coding sequence; 2.9 kb of *THRA*, starting in exon 9 (nucleotide 22889 on Genebank # NC_000077 dark grey box), 3' genomic sequences absent from the recombination vector (black line). White arrows indicate the position and orientation of oligonucleotides used for PCR amplification. The SacII restriction site covers the L400R encoding codon. CRE mediated recombination results in the deletion of the floxed selection cassette, allowing for transcription and translation of the downstream TRα1^{L400R} and TaulacZ reporter protein. B PCR confirmation of homologous recombination in the *THRA* locus in ES cells. Primers a and c amplify a 10.8 kb fragment (2) while h and j amplify 3.3 kb (4) after homologous recombination but not after random DNA integration (1 and 3). C CRE mediated recombination in *TRa^{AMI}*/+ ES cells triggers TRα1^{L400R} expression. RT-PCR of RNA purified from ES cells (primers f and g) amplifies 274 bp of TRα1 cDNA (*) and a non specific product (***). SacII digestion releases two fragments (135bp+139bp **) in ES cells carrying one

CRE-deleted *TRα*^{AMI} allele (3). TRα1^{L400R} expression is not detected in ES cells carrying wild-type alleles (1) or one intact *TRα*^{AMI} allele (2).

Figure 3: phenotype of *TRα*^{AMI}*xS* mice

A *TRα*^{AMI}*xS* mice have lost the *PGKNeopolyA* cassette. PCR was performed on tail DNA with primers b,d,e (Figure 2) amplifying either 1200bp (b+e) for the full length *TRα*^{AMI} allele or 800bp (d+e) for the CRE deleted *TRα*^{AMI} allele. Due to the presence of intronic sequences, the intact *THRA* locus can not be amplified in these conditions. B Body growth reduction in *TRα*^{AMI}*xS* mice compaired to wild-type littermates. Body weight (g) was measured during 80 days (N=22). C Alizarine staining, performed on whole mount skeleton, reveals delayed ossification of long bones (arrow) in *TRα*^{AMI}*xS* mice at P15, clearly visible in posterior limbs. D Delayed cerebellum development in *TRα*^{AMI}*xS* mice: sagital section shows the persistence of the external granular layer (arrows) at P21 in *TRα*^{AMI}*xS* cerebellum (haematoxylin staining) but not in control littermates. E Cold tolerance test: The body temperature of 5 *TRα*^{AMI}*xS* 5-months old adult females (black lines) and 4 control female littermate (grey lines) was recorded during 8 hours of cold exposure. 3 out of 5 animals failed to maintain their body temperature within this time period. F Purkinje cells dendritic arborization, revealed by calbindin-D28k staining, is visible above cell nuclei. The number and size of dendritic spines is reduced at P15 in *TRα*^{AMI}*xS* cerebellum.

Figure 4: Inner ear phenotype of *TRα*^{AMI}*xS* mice

Immunohistochemistry reveals the presence of both prestin and KCNQ4 (red) in wild-type outer hair cells (OHC) at P15. The same observation was performed on 3 *TRα*^{AMI}*xS* mice and 4 wild-type mice. Small arrows underline basolateral staining for prestin, and perinuclear staining for KCNQ4. Vertical arrows indicate the positions of cells nuclei, counterstained with 4',6-diamidino-2-phenylindole (DAPI, blue). Whereas prestin staining is maintained, perinuclear KCNQ4 staining is lost in *TRα*^{AMI}*xS* mice (*).

Figure 5: phenotype of *TRα*^{AMI}*xC* mice

A-D: Phenotype of *TRα*^{AMI}*xC* pups born from females treated with tamoxifen at gestational day 17.5. A: Deletion of the *PGKNeoRpolyA* cassette after tamoxifen treatment at E17.5, analyzed by PCR at P15 (primers b, d, e Figure 2) reveals the presence of a 800bp fragment (*) corresponding to the CRE deleted *TRα*^{AMI} allele in cerebellum (cb) whole brain (wb) and small intestine (si) in *TRα*^{AMI}*xC* mice (+), but not in control littermates without CRE transgene (-). The upper 1200bp band corresponds to the full-length *TRα*^{AMI} allele. B Body weight (g) was measured during 138 days (N=10). Body growth is less affected in *TRα*^{AMI}*xC* mice than in *TRα*^{AMI}*xS* mice (Figure 3B) but significantly reduced compared to *TRα*^{AMI}/+ littermates, which do not express the mutation. C Alizarine staining performed on whole mount skeleton reveals delayed ossification of long bones in *TRα*^{AMI}*xC* mice at P15. The

defect, marked by arrows, is less pronounced than for *TRα^{AMI}xS* mice (Figure 3C). D Persistence of external granular layer in cerebellum at P21. Unlike what is found in wild-type controls, granular precursor cells (black arrow, here in the groove between lobe IV and lobe V) are still present in *TRα^{AMI}xC,* but less abundant than in *TRα^{AMI}xS.* E: Tamoxifen treatment of 8 weeks-old adult males induces a significant decrease (p=0.01 Student t test) of heart rate, measured one week later, in *TRα^{AMI}xC* (N=7) compared to age matched wild-type controls (N=7), also treated with tamoxifen. *TRα^{AMI}xS* data (N=4) are given for comparison.

REFERENCES

1. Yen PM 2001 Physiological and molecular basis of thyroid hormone action. Physiol Rev 81:1097-142
2. Zhang J, Lazar MA 2000 The mechanism of action of thyroid hormones. Annu Rev Physiol 62:439-66
3. Flamant F, Gauthier K, Samarut J 2007 Thyroid hormones signaling is getting more complex: STORMs are coming. Mol Endocrinol 21:321-33
4. Mansouri A, Chowdhury K, Gruss P 1998 Follicular cells of the thyroid gland require Pax8 gene function. Nat Genet 19:87-90.
5. Flamant F, Samarut J 2003 Thyroid hormone receptors: lessons from knockout and knock-in mutant mice. Trends Endocrinol Metab 14:85-90.
6. Tata JR 2006 Amphibian metamorphosis as a model for the developmental actions of thyroid hormone. Mol Cell Endocrinol 246:10-20
7. Plateroti M, Gauthier K, Domon-Dell C, Freund JN, Samarut J, Chassande O 2001 Functional Interference between Thyroid Hormone Receptor alpha (TRalpha) and Natural Truncated TRDeltaalpha Isoforms in the Control of Intestine Development. Mol Cell Biol 21:4761-72.
8. Morte B, Manzano J, Scanlan T, Vennstrom B, Bernal J 2002 Deletion of the thyroid hormone receptor alpha 1 prevents the structural alterations of the cerebellum induced by hypothyroidism. Proc Natl Acad Sci U S A 99:3985-9.
9. Angelin-Duclos C, Domenget C, Kolbus A, Beug H, Jurdic P, Samarut J 2005 Thyroid hormone T3 acting through the thyroid hormone alpha receptor is necessary for implementation of erythropoiesis in the neonatal spleen environment in the mouse. Development 132:925-34
10. O'Shea P J, Bassett JH, Cheng SY, Williams GR 2006 Characterization of skeletal phenotypes of TRalpha1 and TRbeta mutant mice: implications for tissue thyroid status and T3 target gene expression. Nucl Recept Signal 4:e011
11. Gloss B, Trost S, Bluhm W, Swanson E, Clark R, Winkfein R, Janzen K, Giles W, Chassande O, Samarut J, Dillmann W 2001 Cardiac ion channel expression and contractile function in mice with deletion of thyroid hormone receptor alpha or beta. Endocrinology 142:544-50
12. Gothe S, Wang Z, Ng L, Kindblom JM, Barros AC, Ohlsson C, Vennstrom B, Forrest D 1999 Mice devoid of all known thyroid hormone receptors are viable but exhibit disorders of the pituitary-thyroid axis, growth, and bone maturation. Genes Dev 13:1329-41
13. Gauthier K, Chassande O, Plateroti M, Roux JP, Legrand C, Pain B, Rousset B, Weiss R, Trouillas J, Samarut J 1999 Different functions for the thyroid hormone receptors TRalpha and TRbeta in the control of thyroid hormone production and post-natal development. Embo J 18:623-31
14. Flamant F, Poguet AL, Plateroti M, Chassande O, Gauthier K, Streichenberger N, Mansouri A, Samarut J 2002 Congenital Hypothyroid Pax8(-/-) Mutant Mice Can Be Rescued by Inactivating the TRalpha Gene. Mol Endocrinol 16:24-32.
15. Tinnikov A, Nordstrom K, Thoren P, Kindblom JM, Malin S, Rozell B, Adams M, Rajanayagam O, Pettersson S, Ohlsson C, Chatterjee K, Vennstrom B 2002 Retardation of

post-natal development caused by a negatively acting thyroid hormone receptor alpha1. Embo J 21:5079-87
16. Itoh Y, Esaki T, Kaneshige M, Suzuki H, Cook M, Sokoloff L, Cheng SY, Nunez J 2001 Brain glucose utilization in mice with a targeted mutation in the thyroid hormone alpha or beta receptor gene. Proc Natl Acad Sci U S A 98:9913-8.
17. Kaneshige M, Suzuki H, Kaneshige K, Cheng J, Wimbrow H, Barlow C, Willingham MC, Cheng Sy S 2001 A targeted dominant negative mutation of the thyroid hormone alpha 1 receptor causes increased mortality, infertility, and dwarfism in mice. Proc Natl Acad Sci U S A 98:15095-100
18. Liu YY, Tachiki KH, Brent GA 2002 A targeted thyroid hormone receptor alpha gene dominant-negative mutation (P398H) selectively impairs gene expression in differentiated embryonic stem cells. Endocrinology 143:2664-72.
19. Mittag J, Friedrichsen S, Heuer H, Polsfuss S, Visser TJ, Bauer K 2005 Athyroid Pax8-/- Mice Cannot Be Rescued by the Inactivation of Thyroid Hormone Receptor {alpha}1. Endocrinology 146:3179-84
20. Hashimoto K, Curty FH, Borges PP, Lee CE, Abel ED, Elmquist JK, Cohen RN, Wondisford FE 2001 An unliganded thyroid hormone receptor causes severe neurological dysfunction. Proc Natl Acad Sci U S A 98:3998-4003.
21. Farwell AP, Dubord-Tomasetti SA, Pietrzykowski AZ, Leonard JL 2006 Dynamic Non-Genomic Actions Of Thyroid Hormone In The Developing Rat Brain. Endocrinology 147:2567-2574
22. Davis PJ, Davis FB, Cody V 2005 Membrane receptors mediating thyroid hormone action. Trends Endocrinol Metab
23. Darimont BD, Wagner RL, Apriletti JW, Stallcup MR, Kushner PJ, Baxter JD, Fletterick RJ, Yamamoto KR 1998 Structure and specificity of nuclear receptor-coactivator interactions. Genes Dev 12:3343-56
24. Feng W, Ribeiro RC, Wagner RL, Nguyen H, Apriletti JW, Fletterick RJ, Baxter JD, Kushner PJ, West BL 1998 Hormone-dependent coactivator binding to a hydrophobic cleft on nuclear receptors. Science 280:1747-9
25. Nascimento AS, Dias SM, Nunes FM, Aparicio R, Ambrosio AL, Bleicher L, Figueira AC, Santos MA, de Oliveira Neto M, Fischer H, Togashi M, Craievich AF, Garratt RC, Baxter JD, Webb P, Polikarpov I 2006 Structural rearrangements in the thyroid hormone receptor hinge domain and their putative role in the receptor function. J Mol Biol 360:586-98
26. Chung SS, Cuzin F, Rassoulzadegan M, Wolgemuth DJ 2004 Primary spermatocyte-specific Cre recombinase activity in transgenic mice. Transgenic Res 13:289-94
27. Golozoubova V, Gullberg H, Matthias A, Cannon B, Vennstrom B, Nedergaard J 2004 Depressed thermogenesis but competent brown adipose tissue recruitment in mice devoid of all hormone-binding thyroid hormone receptors. Mol Endocrinol 18:384-401
28. Winter H, Braig C, Zimmermann U, Geisler HS, Franzer JT, Weber T, Ley M, Engel J, Knirsch M, Bauer K, Christ S, Walsh EJ, McGee J, Kopschall I, Rohbock K, Knipper M 2006 Thyroid hormone receptors TRalpha1 and TRbeta differentially regulate gene expression of Kcnq4 and prestin during final differentiation of outer hair cells. J Cell Sci 119:2975-84
29. Hayashi S, McMahon AP 2002 Efficient recombination in diverse tissues by a tamoxifen-inducible form of Cre: a tool for temporally regulated gene activation/inactivation in the mouse. Dev Biol 244:305-18
30. Lavado-Autric R, Auso E, Garcia-Velasco JV, Arufe Mdel C, Escobar del Rey F, Berbel P, Morreale de Escobar G 2003 Early maternal hypothyroxinemia alters histogenesis and cerebral cortex cytoarchitecture of the progeny. J Clin Invest 111:1073-82
31. Garcia-Otin AL, Guillou F 2006 Mammalian genome targeting using site-specific recombinases. Front Biosci 11:1108-36
32. Gullberg H, Rudling M, Salto C, Forrest D, Angelin B, Vennstrom B 2002 Requirement for thyroid hormone receptor Beta in t(3) regulation of cholesterol metabolism in mice. Mol Endocrinol 16:1767-77.

33. Plateroti M, Chassande O, Fraichard A, Gauthier K, Freund JN, Samarut J, Kedinger M 1999 Involvement of T3Ralpha- and beta-receptor subtypes in mediation of T3 functions during postnatal murine intestinal development. Gastroenterology 116:1367-78
34. Arpin C, Pihlgren M, Fraichard A, Aubert D, Samarut J, Chassande O, Marvel J 2000 Effects of T3R alpha 1 and T3R alpha 2 gene deletion on T and B lymphocyte development. J Immunol 164:152-60
35. Johansson C, Lannergren J, Lunde PK, Vennstrom B, Thoren P, Westerblad H 2000 Isometric force and endurance in soleus muscle of thyroid hormone receptor-alpha(1)- or -beta-deficient mice. Am J Physiol Regul Integr Comp Physiol 278:R598-603
36. Rodriguez-Pena A, Ibarrola N, Iniguez MA, Munoz A, Bernal J 1993 Neonatal hypothyroidism affects the timely expression of myelin-associated glycoprotein in the rat brain. J Clin Invest 91:812-8.
37. Voinesco F, Glauser L, Kraftsik R, Barakat-Walter I 1998 Local administration of thyroid hormones in silicone chamber increases regeneration of rat transected sciatic nerve. Exp Neurol 150:69-81
38. Knipper M, Zinn C, Maier H, Praetorius M, Rohbock K, Kopschall I, Zimmermann U 2000 Thyroid hormone deficiency before the onset of hearing causes irreversible damage to peripheral and central auditory systems. J Neurophysiol 83:3101-12.
39. Lemkine GF, Raj A, Alfama G, Turque N, Hassani Z, Alegria-Prevot O, Samarut J, Levi G, Demeneix BA 2005 Adult neural stem cell cycling in vivo requires thyroid hormone and its alpha receptor. Faseb J 19:863-5
40. Montero-Pedrazuela A, Venero C, Lavado-Autric R, Fernandez-Lamo I, Garcia-Verdugo JM, Bernal J, Guadano-Ferraz A 2006 Modulation of adult hippocampal neurogenesis by thyroid hormones: implications in depressive-like behavior. Mol Psychiatry
41. Venero C, Guadano-Ferraz A, Herrero AI, Nordstrom K, Manzano J, de Escobar GM, Bernal J, Vennstrom B 2005 Anxiety, memory impairment, and locomotor dysfunction caused by a mutant thyroid hormone receptor {alpha}1 can be ameliorated by T3 treatment. Genes Dev 19:2152-63
42. Ying H, Araki O, Furuya F, Kato Y, Cheng SY 2007 Impaired adipogenesis caused by a mutated thyroid hormone {alpha} 1 receptor. Mol Cell Biol
43. Esaki T, Suzuki H, Cook M, Shimoji K, Cheng SY, Sokoloff L, Nunez J 2003 Functional activation of cerebral metabolism in mice with mutated thyroid hormone nuclear receptors. Endocrinology 144:4117-22
44. Liu YY, Heymann RS, Moatamed F, Schultz JJ, Sobel D, Brent GA 2006 A Mutant Thyroid Hormone Receptor {alpha} Antagonizes PPAR{alpha}-Signaling In Vivo and Impairs Fatty Acid Oxidation. Endocrinology
45. Liu YY, Heymann RS, Moatamed F, Schultz JJ, Sobel D, Brent GA 2007 A mutant thyroid hormone receptor alpha antagonizes peroxisome proliferator-activated receptor alpha signaling in vivo and impairs fatty acid oxidation. Endocrinology 148:1206-17
46. Farwell AP, Dubord-Tomasetti SA, Pietrzykowski AZ, Stachelek SJ, Leonard JL 2005 Regulation of cerebellar neuronal migration and neurite outgrowth by thyroxine and 3,3',5'-triiodothyronine. Brain Res Dev Brain Res 154:121-35
47. Forrest D, Vennstrom B 2000 Functions of thyroid hormone receptors in mice. Thyroid 10:41-52
48. Marrif H, Schifman A, Stepanyan Z, Gillis MA, Calderone A, Weiss RE, Samarut J, Silva JE 2005 Temperature Homeostasis in transgenic mice lacking thyroid hormone receptor alpha gene products. Endocrinology
49. Wikstrom L, Johansson C, Salto C, Barlow C, Campos Barros A, Baas F, Forrest D, Thoren P, Vennstrom B 1998 Abnormal heart rate and body temperature in mice lacking thyroid hormone receptor alpha 1. Embo J 17:455-61.
50. Ribeiro MO, Carvalho SD, Schultz JJ, Chiellini G, Scanlan TS, Bianco AC, Brent GA 2001 Thyroid hormone--sympathetic interaction and adaptive thermogenesis are thyroid hormone receptor isoform--specific. J Clin Invest 108:97-105
51. Hernandez A, Obregon MJ 1996 Presence and mRNA expression of T3 receptors in differentiating rat brown adipocytes. Mol Cell Endocrinol 121:37-46

52. Nicholson JL, Altman J 1972 The effects of early hypo- and hyperthyroidism on the development of the rat cerebellar cortex. II. Synaptogenesis in the molecular layer. Brain Res 44:25-36.
53. Bradley DJ, Young WS, 3rd, Weinberger C 1989 Differential expression of alpha and beta thyroid hormone receptor genes in rat brain and pituitary. Proc Natl Acad Sci U S A 86:7250-4.
54. Heuer H, Mason CA 2003 Thyroid hormone induces cerebellar Purkinje cell dendritic development via the thyroid hormone receptor alpha1. J Neurosci 23:10604-12
55. Forrest D, Hallbook F, Persson H, Vennstrom B 1991 Distinct functions for thyroid hormone receptors alpha and beta in brain development indicated by differential expression of receptor genes. Embo J 10:269-75.
56. Billon N, Jolicoeur C, Tokumoto Y, Vennstrom B, Raff M 2002 Normal timing of oligodendrocyte development depends on thyroid hormone receptor alpha 1 (TRalpha1). Embo J 21:6452-6460.
57. Kmita M, Tarchini B, Duboule D, Herault Y 2002 Evolutionary conserved sequences are required for the insulation of the vertebrate Hoxd complex in neural cells. Development 129:5521-8
58. Mombaerts P, Wang F, Dulac C, Chao SK, Nemes A, Mendelsohn M, Edmondson J, Axel R 1996 Visualizing an olfactory sensory map. Cell 87:675-86
59. Lee S, Privalsky ML 2005 Heterodimers of retinoic Acid receptors and thyroid hormone receptors display unique combinatorial regulatory properties. Mol Endocrinol 19:863-78
60. Livak JL, Schmittgen TD 2001 Analysis of relative gene expression data using real-time quantitative PCR and the 2-DDCT method. Methods 25:402-408
61. Weiss RE, Forrest D, Pohlenz J, Cua K, Curran T, Refetoff S 1997 Thyrotropin regulation by thyroid hormone in thyroid hormone receptor beta-deficient mice. Endocrinology 138:3624-9

Mouse genotype		+/+	$TR\alpha^{AMI}$/+	$TR\alpha^{AMI}xS$	$TR\alpha^{AMI}xC$*
Physiological parameters P15					
Serum T4 (µg/dL)		9,3±0,6	9,6±1	9,0±2,4	6,8±2,2**
Serum T3 (ng/dL)		141±22	168±15	129±13	164±8
Spleen weight (mg)		39,5±9,1	45,0±10,8	26,9±12,2***	26,2±7,5**
Physiological parameters in adult males (2 – 3 months)					
Serum T4 (µg/dL)		4,3±0,8	ND	4,2±0,7	ND
Serum T3 (ng/dL)		116±24	ND	123±12	ND
Serum TSH (mU/L) †		144±106	ND	50±26	ND
Heart beat (/min) †		393±45	ND	224±24***	ND
Body temperature (°C)		38,3±0,4	38,6±0,2	38,5±0,4	38,4±0,5
Body fat content (%)†		9,33±1,61	ND	8,20±0,36	ND
Gene expression P15 (% of wild type)					
Gene	Tissue/organ				
GH	pituitary	100±47	142±33	44±20**	52±18
TSHβ	pituitary	100±31	171±53**	65±32	120±12
Dio1	liver	100±17	112±26	101±51	ND
ME3	Liver	100±38	86±17	130±20	ND
$TR\alpha1+TR\alpha1^{L400R}$	liver	100±12	71±15**	94±6	81±13
HCN2	heart	100±27	76±32	7±2***	5±2***
KCNB1	heart	100±18	87±24	25±6***	21±7***
Hr	cerebellum	100±19	132±37	19±5***	39±11***
PcP2	cerebellum	100±21	122±21	38±21***	105±10
$TR\alpha1+TR\alpha1^{L400R}$	cerebellum	100±26	140±29**	327±48***	374±56***

* tamoxifen treated at E17.5 ** different from wild type, $p < 0,05$ *** $p < 0,01$ ND = Not Determined †Males only

A

	SRC1		SRC2		NcoR	
T3	–	+	–	+	–	+
TRα1	–	+	–	+	+	–
$TR\alpha1^{L400R}$	–	–	–	–	+	+

B

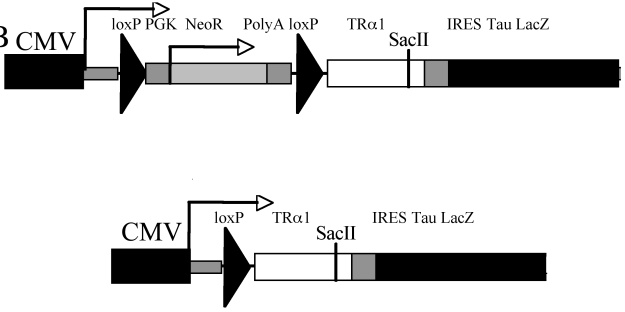

C

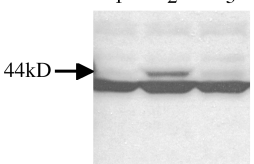

D

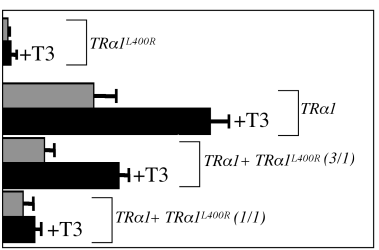

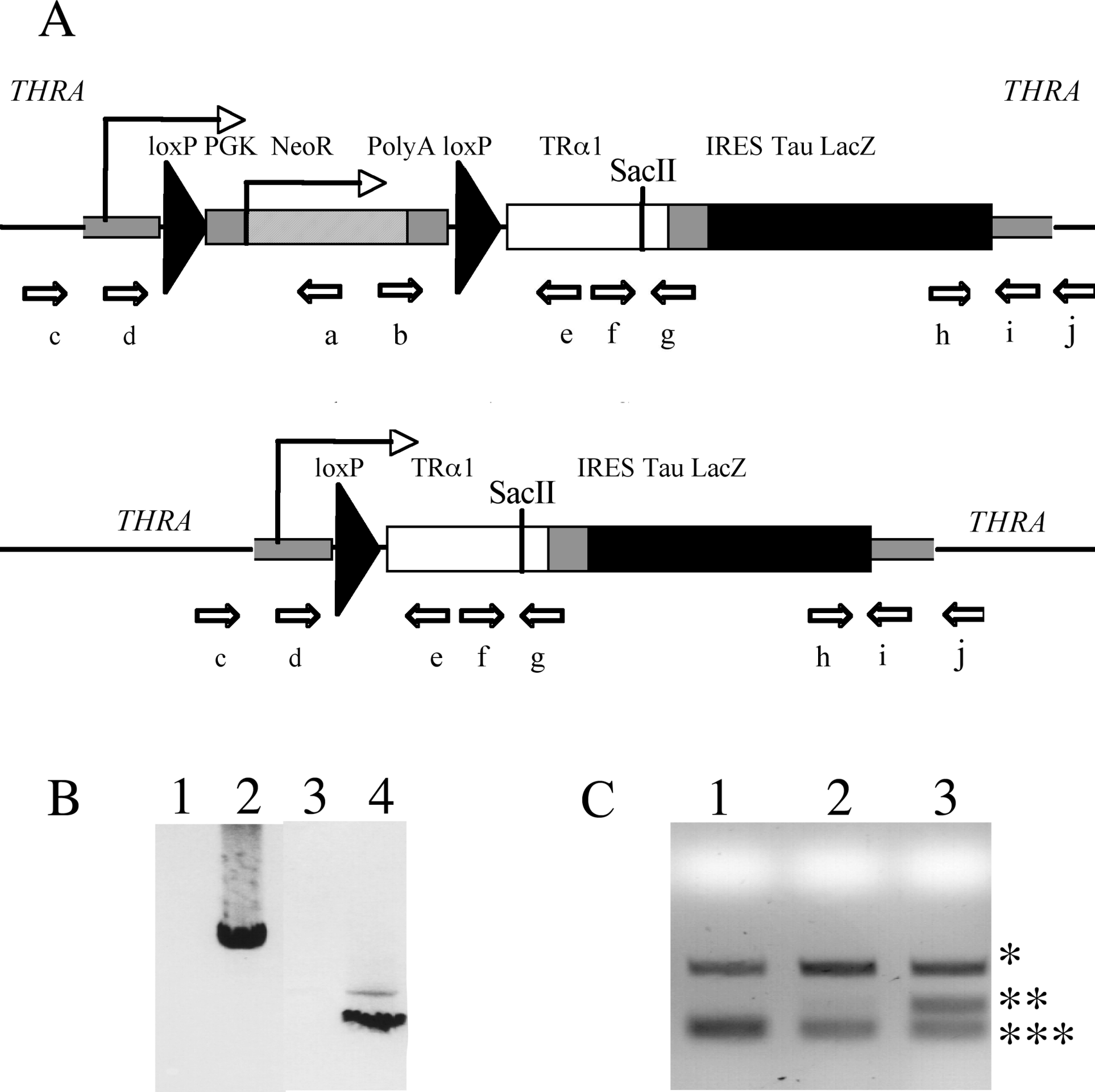
A
THRA
THRA
loxP PGK NeoR
PolyA loxP
TRα1
IRES Tau LacZ
SacII
c
d
a
b
e
f
g
h
i
j
loxP
TRα1
IRES Tau LacZ
SacII
THRA
THRA
c
d
e
f
g
h
i
j
B
1 2 3 4
C
1 2 3
*
**
***

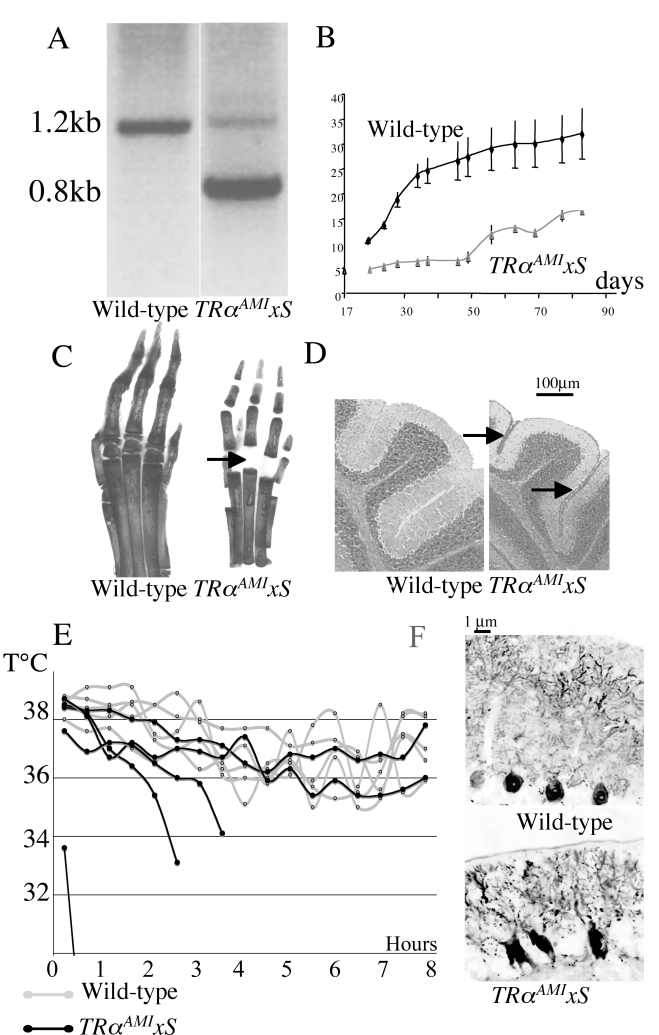
A
1.2kb
0.8kb
Wild-type TRα^AMIxS
B
Wild-type
TRα^AMIxS
days
17
30
50
70
90
C
Wild-type TRα^AMIxS
D
100µm
Wild-type TRα^AMIxS
E
T°C
38
36
34
32
Hours
0
1
2
3
4
5
6
7
8
Wild-type
TRα^AMIxS
F
1 µm
Wild-type
TRα^AMIxS

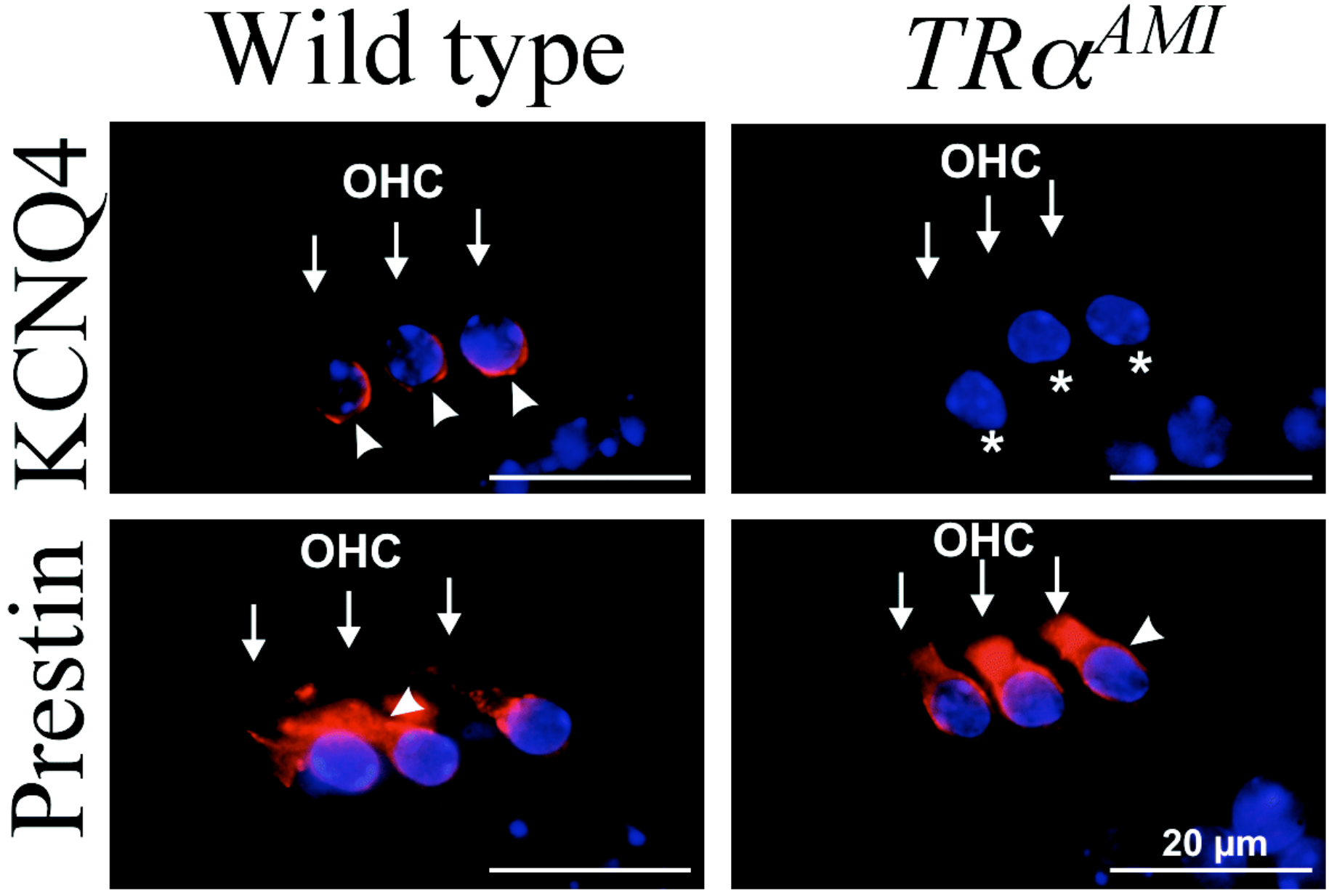
Wild type
TRα^AMI
KCNQ4
Prestin
OHC
OHC
OHC
OHC
20 µm

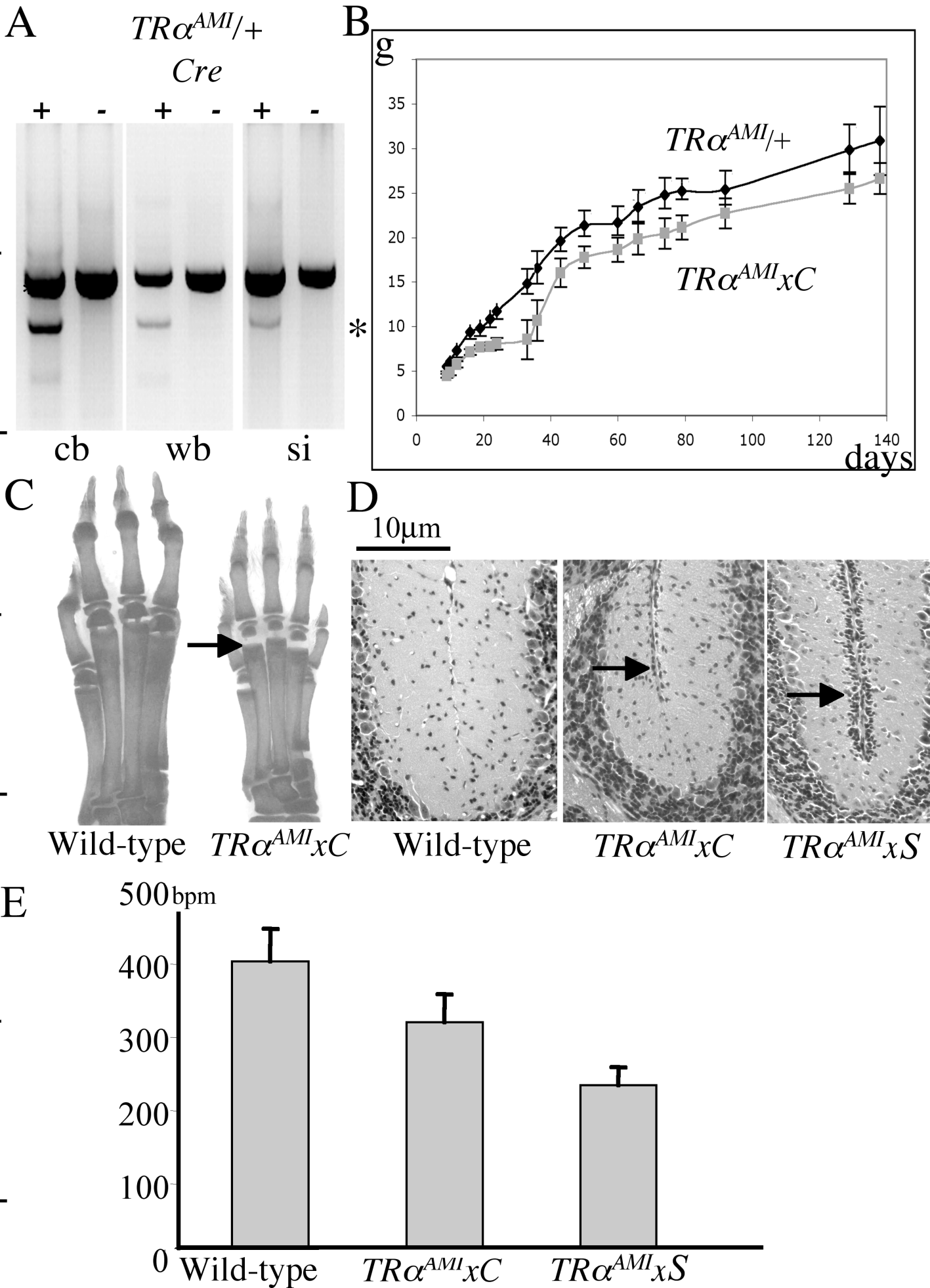
A
TRα^AMI/+
Cre
+ - + - + -
cb
wb
si
B
g
35
30
25
20
15
10
5
0
0 20 40 60 80 100 120 140
days
TRα^AMI/+
TRα^AMIxC
*
C
Wild-type
TRα^AMIxC
D
10μm
Wild-type
TRα^AMIxC
TRα^AMIxS
E
500 bpm
400
300
200
100
0
Wild-type
TRα^AMIxC
TRα^AMIxS